W.R.B. de Araújo, J.P.B.C.de Melo, K. Tsushima
Study of the in-medium nucleon electromagnetic form factors using a light-front nucleon wave function combined with the quark-meson coupling model
Nuclear Physics A, 2018; 970:325-352

Published at: http://dx.doi.org/10.1016/j.nuclphysa.2017.12.005

LFTC-17-5/5

Medium modifications of the nucleon electromagnetic form factors in a light-front approach

W. R. B. de Araújo[a], J. P. B. C. de Melo[b], K. Tsushima[b]

[a] *Secretaria de Educação do Estado de São Paulo, DE Norte 2, São Paulo, SP, Brazil. and*

[b] *Laboratório de Física Teórica e Computacional, Universidade Cruzeiro do Sul, 01506-000, São Paulo, SP, Brazil*

(Dated: July 4, 2017)

Abstract

We study the nucleon electromagnetic form factors in a nuclear medium as well as in vacuum, within a light-front approach with the in-medium input calculated by the quark-meson coupling model. The same in-medium quark properties are used as those already used for the study of in-medium pion properties. The zero of the proton electromagnetic form factor ratio in vacuum, namely, the electric to magnetic form factors, $\mu_p G_{Ep}(Q^2)/G_{Mp}(Q^2)$ ($Q^2 = -q^2 > 0$, q the four-momentum transfer), is determined including the latest experimental data, by implementing a hard constituent quark component in the nucleon wave function. A reasonable fit is achieved for the ratio $\mu_p G_{Ep}(Q^2)/G_{Mp}(Q^2)$ in vacuum, and we predict the Q_0^2 value to cross the zero of the ratio, to be about 15 GeV^2. In addition, the double ratio data of the proton electromagnetic form factors in ^{4}He and H nuclei, $[G_{Ep}^{^4\mathrm{He}}(Q^2)/G_{Mp}^{^4\mathrm{He}}(Q^2)]/[G_{Ep}^{^1\mathrm{H}}(Q^2)/G_{Mp}^{^1\mathrm{H}}(Q^2)]$, the data extracted by the polarized $(\vec{e}, e'\vec{p})$ scattering experiment on ^{4}He at JLab, are well described. We also predict the Q_0^2 value for $\mu_p G_{Ep}(Q_0^2)/G_{Mp}(Q_0^2) = 0$ in a nuclear medium, shifts to a smaller value as increasing nuclear density.

PACS numbers: 24.85.+p, 21.65.-f, 14.20.Dh, 13.40.Gp, 12.39.-x

I. INTRODUCTION

One of the most challenging and exciting topics in hadronic and nuclear physics is how the hadron properties are modified in a nuclear medium (nuclear environment), and how such modifications can be measured in experiment. Since hadrons are composed of quarks, antiquarks and gluons, it is natural to expect that the hadron internal structure is modified when they are immersed in a nuclear medium and in atomic nuclei [1–6]. At sufficiently high nuclear density and/or temperature, there is no doubt that the quark and gluon degrees of freedom are the correct degrees of freedom to describe the properties of hadrons according to quantum chromodynamics (QCD). On the other hand, it is also true that effective description of hadronic and nuclear processes is very successful by means of the meson and baryon degrees of freedom, especially in a lower energy and temperature region. Although there is hope that lattice QCD simulation eventually can describe consistently the properties of hadrons in a nuclear medium as well as nucleus itself, the current status seems still difficult to get a reliable result at finite nuclear density [7, 8].

To understand the deep inelastic scattering (DIS) data at momentum transfer of several GeV, one certainly needs explicit quark degrees of freedom [9–11]. In particular, the nuclear EMC effect [12, 13] has suggested the necessity of including the degrees of freedom beyond the traditional nucleon and mesons. Furthermore, there is strong implication for the modification of the bound proton electromagnetic form factors in the measurement of the double ratio of proton-recoil polarization transfer coefficients in $(\vec{e}, e'\vec{p})$ scattering experiments on ^{16}O and ^{4}He nuclei at MAMI and JLab [14–16]. It is also clear that the properties of bound neutron is modified in a nucleus, since it becomes stable, while the free neutron mean life is about 880 seconds due to the beta decay emitting a proton and an antineutrino.

However, it is very difficult to unambiguously separate and identify the observed effects by the relevant degrees of freedom. In particular, to distinguish the possible in-medium modifications due to the nucleon internal structure change in a nuclear medium [17–20], from those due to the conventional many-body effects, such as the final state interactions and meson exchange effects described at the hadronic degrees of freedom [21]. Such separation may only be possible in a model dependent manner, since general experimental data involve all the effects simultaneously. Thus, the interpretation of the modifications observed in experiments has not yet been established.

In this article, we study the modification of the nucleon electromagnetic form factors in symmetric nuclear matter, focusing on the internal structure change of nucleon. Namely, we study the nucleon electromagnetic form factors in nuclear matter arising from the property change of the light quarks inside the nucleon, using the in-medium input calculated by the quark-meson coupling (QMC) model [3, 22]. The QMC model has been successfully applied for various nuclear and hadronic reactions and processes. A similar approach as in the present study was already applied for the study of pion properties in nuclear matter [23–26]. Although there may be possible to have alternative explanations based on traditional nuclear physics approaches, our interest of this study is on the internal structure change of nucleon in a nuclear medium.

For this purpose, we rely on a light-front model of nucleon in vacuum, the "relativistic quark-spin coupling" model [27, 28], which was used for studying the nucleon electromagnetic and axial-vector form factors in vacuum with some extension [28]. This model can keep close connection with covariant field theory, and perform a three-dimensional reduction for the photo-absorption amplitude with the nucleon in the null-plane, $x^+ = x^0 + x^3 = 0$. After the three-dimensional reduction, one can introduce the nucleon light-front wave function in the two-loop momentum integrations. For studying the nucleon electromagnetic form factors, the "triangle diagrams" with an impulse approximation is used. In Ref. [27] the hard-scale component in the nucleon wave function was firstly introduced to improve the description of the zero of the proton electromagnetic form factor ratio, $\mu_p G_{Ep}(Q^2)/G_{Mp}(Q^2)$ ($Q^2 = -q^2 > 0$, q the four-momentum transfer). In addition a detailed study was made for the different quark-spin coupling effects in Refs. [27, 28]. It turned out that the neutron electric form factor can strongly constrain the quark-spin coupling in the nucleon wave function, and the model preferred the scalar-pair coupling. Furthermore, to describe the zero of the proton electromagnetic form factor ratio, the introduction of the hard-scale component in the nucleon wave function was crucial. Thus, we use the two-scale model of the nucleon wave function in vacuum with the scalar-pair coupling, and study the medium modification of the nucleon electromagnetic form factors.

We predict the Q_0^2 value to cross the zero of the ratio, $\mu_p G_{Ep}(Q_0^2)/G_{Mp}(Q_0^2) = 0$, to be about 15 GeV^2. Furthermore the double ratio data of the proton electromagnetic form factors in ^{4}He and H nuclei, $[G_{Ep}^{^4\mathrm{He}}(Q^2)/G_{Mp}^{^4\mathrm{He}}(Q^2)]/[G_{Ep}^{^1\mathrm{H}}(Q^2)/G_{Mp}^{^1\mathrm{H}}(Q^2)]$, the data extracted by the polarized $(\vec{e}, e'\vec{p})$ scattering experiment on ^{4}He at JLab, turn out to be well described.

We also predict the Q_0^2 value of $\mu_p G_{Ep}(Q_0^2)/G_{Mp}(Q_0^2) = 0$ in a nuclear medium, shifts to a smaller value as increasing nuclear density.

The organization of this article is as follows. In Sec. II, we explain the relativistic quark-spin coupling model of nucleon, two scale-model as well as nucleon electromagnetic form factors in light-front approach, and present the nucleon electromagnetic form factors in vacuum. In Sec. III we review properties of nuclear medium necessary to study the in-medium modification of the nucleon electromagnetic form factors, the QMC model, and discuss the in-medium input. We present main results of this study, the in-medium nucleon electromagnetic form factors in Sec. IV. Finally, we give summary and discussions in Sec. V.

II. NUCLEON ELECTROMAGNETIC FORM FACTORS IN VACUUM

Here, we briefly review a light-front approach for the nucleon structure, the relativistic quark-spin coupling model, and the two-scale model [27]. The effective Lagrangian for the quark-spin coupling in the nucleon [27–29], accounts for calculating the static electromagnetic observables with a totally symmetric momentum component of the nucleon wave function. However, the initial version of the model was necessary to be improved to describe better the zero of $\mu_p G_{Ep}(Q^2)/G_{Mp}(Q^2)$ [30–37], namely, the position of the zero to be shifted to a larger Q^2. The effective Lagrangian for the three constituent quarks coupled to form the nucleon wave function is given by,

$$\mathcal{L}_{\rm N-3q} = m_N \epsilon^{lmn} \overline{\Psi}_{(l)} i\tau_2\gamma_5 \Psi^C_{(m)} \overline{\Psi}_{(n)} \Psi_N + H.C., \tag{1}$$

where τ_2 is the Pauli matrix operating in isospin space, and the color indices are $\{l, m, n\}$ with ϵ^{lmn} being the totally antisymmetric tensor. The conjugate quark field is $\Psi^C = C\overline{\Psi}^T$ with $C = i\gamma^2\gamma^0$, the charge conjugation matrix, and T stands for transposition.

The momentum scale of the nucleon wave function for Gaussian and power law shapes with constituent light-quark mass $m_q = 0.22$ GeV, was found to be about 0.6 - 0.8 GeV from the fit to the nucleon magnetic moments and mean square-charge radii [27]. (We note that the same value of the light-quark constituent mass $m_q = 0.22$ GeV was also used for the studies of pion properties in vacuum [38], as well as in medium [23–26].) It turned out that the neutron electric form factor can constrain the relativistic quark-spin coupling scheme, and the scalar-pair coupling in the effective Lagrangian is preferred.

However, although the effective Lagrangian approach to the quark-spin coupling allows a reasonable account for the static nucleon electromagnetic observables with a totally symmetric momentum component of the nucleon wave function, it has a too small momentum scale which leads to too small value for the zero of $\mu_p G_{Ep}(Q^2)/G_{Mp}(Q^2)$ [20, 27] than that the experimental data imply [30–37].

Therefore within this approach, one is led to introduce another term in the momentum component of the nucleon wave function, which would represent a higher-momentum scale, to be able to describe better the zero of $\mu_p G_{Ep}(Q^2)/G_{Mp}(Q^2)$ without destroying the good description achieved in the lower momentum transfer region [27, 28].

In some light-front models applied to mesons [39–46], a high-momentum scale appears naturally associated with the short-range interaction between the constituent quarks. A reasonable description of the meson spectrum and pion properties was achieved including a Dirac-delta interaction in the mass-squared operator [39–41], inspired by the hyperfine interaction from the effective one-gluon exchange between the constituent quarks [39, 47]. The model [41] reveals some of the physics contained in the observation of the trajectories of mesons in the (n, M^2)-plane, that are almost linear [48, 49]. The model naturally incorporates the small pion mass as a consequence of the short-range attraction in the spin-zero channel, which is also responsible for the pion and rho-meson mass splitting [41].

The short-range attractive part of the quark-quark interaction which is presented in the Godfrey and Isgur model [50], generates a high-momentum component as well in the light-cone pion wave function above the energy 1 GeV, and was successfully able to describe the electroweak structure of pion [51]. Nonetheless, it was pointed out that the existing electroweak data were not enough to draw a definite conclusion about the presence of the hard-constituent quarks in the hadron wave function [52]. Recently, this discussion led to a new insight when the valence-quark light-cone momentum distribution was probed in the experiment of diffractive dissociation of 500-GeV π^- into dijets [53], which supports the importance of the asymptotic part of the wave function [54], and the presence of a high-momentum component in the pion wave function [40].

Motivated by the above discussions which indicate the necessity of a strong short-range attractive interaction in the spin-zero channel and a high-momentum tail in the pion valence component in the wave function, we introduce a high-momentum component in the valence nucleon wave function. We study the role of this high-momentum component in the

calculation of the nucleon electromagnetic form factors. Indeed, the quality of the model description including the recent data for $\mu_p G_{Ep}(Q^2)/G_{Mp}(Q^2)$, is improved substantially as we show later.

Thus, we use the "two-scale model", which includes the high-momentum component in the nucleon wave function in a light-front approach, in an effective Lagrangian with the spin coupling between the quarks Eq. (1) in a scalar form. Furthermore, we choose a power-law form [47, 55] for the momentum component of the nucleon wave function,

$$\Psi_{\rm Power} = N_{\rm Power}\left[(1+M_0^2/\beta^2)^{-p} + \lambda(1+M_0^2/\beta_1^2)^{-p}\right] \ , \tag{2}$$

$$\lambda = \left[(1+M_H^2/\beta_1^2)/(1+M_H^2/\beta^2)\right]^p \ , \tag{3}$$

which preserves the asymptotic behavior suggested by QCD. The normalization constant $N_{\rm Power}$ above is determined by the proton charge. The characteristic momentum scales of the wave function are represented by β, β_1 and M_H, while M_0 is the free mass of the three-quark system, and its explicit expression is given in Ref. [27]. The lower momentum scale is essentially determined by the nucleon static observables, while the higher one is related with the zero of $G_{Ep}(Q^2)$. A possible definition of the high-momentum scale brought by Eq. (2) is the value of M_0 at which the two terms are equal, therefore one easily gets,

$$\beta_H = \beta\beta_1\left(\frac{1-|\lambda|^{\frac{1}{3}}}{\beta_1^2|\lambda|^{\frac{1}{3}}-\beta^2}\right)^{\frac{1}{2}} \ . \tag{4}$$

We stress that this value should be interpreted as a guiding reference. Note that the asymptotic behavior of Eq. (2) does not depend on the parameters. The totally symmetric forms of Eq. (2), due to the relativistic spin-coupling coefficients which depend on momentum, effectively lead to the breaking of the SU(6) flavor symmetry as discussed in Ref. [56].

The falloff based on perturbative QCD arguments for the power-low, has a value of $p = 3.5$ in Eq. (2) [47, 55]. From the point of view of the static electroweak observables, the value of p does not present an independent feature, once one static observable is fitted. Namely, the other parameters in Eq. (2) are strongly correlated, as long as $p > 2$ [27, 55]. In this study, we choose $p = 3$.

The light-front formulation of the nucleon electroweak form factors in Ref. [27] uses the effective Lagrangian Eq. (1), to construct the coupling of the quark spin in the valence component of the nucleon wave function. The form factor calculation is made by an impulse

approximation defined within a covariant field theory. The nucleon virtual photon absorption amplitude is projected on the three-dimensional hypersurface, $x^+ = x^0 + x^3 = 0$ (see, e.g., Ref. [57]).

The elimination of the relative light-front time between the particles in favor of the global time propagation [58], comes from the analytical integration in the individual light-front energies ($k^- = k^0 - k^3$) in the two-loop amplitude. Then, the momentum component of the nucleon light-front wave function is introduced into the remaining form of the two-loop three-dimensional momentum integrations which define the matrix elements of the electroweak currents [27, 59, 60].

The plus component of the nucleon electromagnetic current ($J_N^+ = J_N^0 + J_N^3$) for momentum transfers satisfying the Drell-Yan condition $q^+ = q^0 + q^3 = 0$, is used to calculate the electromagnetic form factors. The contribution of the Z-diagram is minimized in a Drell-Yan frame, while the wave function contribution to the current is maximized [47, 57, 59–61]. We use the Breit-frame, where the four-momentum transfer $q = (0, \vec{q}_\perp, 0)$ is such that $(q^+ = 0)$ and $\vec{q}_\perp = (q^1, q^2)$, satisfying the Drell-Yan condition.

The nucleon electromagnetic form factors are calculated with the matrix elements of the current $J_N^+(Q^2)$ in the light-front spinor basis in the Breit-frame with the Drell-Yan condition [27, 62]. The Dirac and Pauli form factors are respectively given by,

$$\begin{aligned} F_{1N}(Q^2) &= \frac{1}{\sqrt{1+\eta}} \langle N \uparrow | J_N^+(Q^2) | N \uparrow \rangle \ , \\ F_{2N}(Q^2) &= \frac{1}{\sqrt{\eta}\sqrt{1+\eta}} \langle N \uparrow | J_N^+(Q^2) | N \downarrow \rangle \ , \end{aligned} \tag{5}$$

where $\eta = Q^2/4m_N$. The momentum transfer in the Breit-frame is chosen along the x-direction, i.e., $\vec{q_\perp} = (\sqrt{Q^2}, 0)$.

The nucleon electric and magnetic form factors (Sachs form factors) are given by:

$$\begin{aligned} G_{EN}(Q^2) &= F_{1N}(Q^2) - \frac{Q^2}{4m_N^2} F_{2N}(Q^2) \ , \\ G_{MN}(Q^2) &= F_{1N}(Q^2) + F_{2N}(Q^2) \ , \end{aligned} \tag{6}$$

with $N =$ p or n. $\mu_N = G_{MN}(0)$ is the magnetic moment and $\kappa_N = F_{2N}(0)$ is the anomalous one. The charge mean square radius is calculated by $r_N^2 = -6 \frac{dG_{EN}(Q^2)}{dQ^2}|_{Q^2=0}$.

The microscopic matrix elements of the nucleon electromagnetic current are derived from the effective Lagrangian, Eq. (1), within the light-front impulse approximation which is rep-

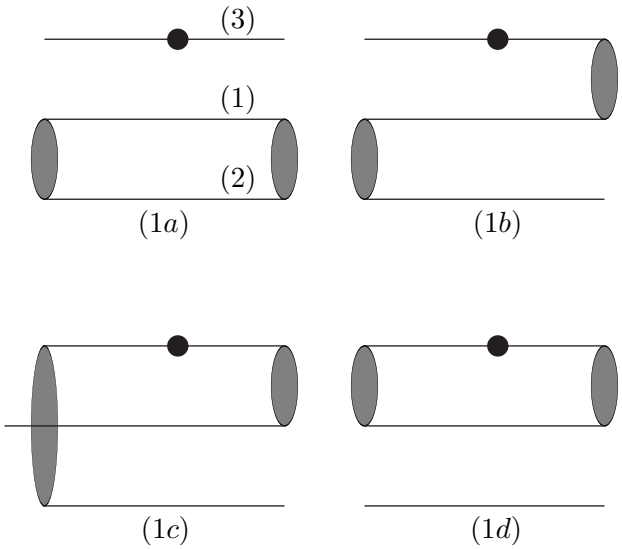

FIG. 1: Diagrammatic representation of the nucleon photo-absorption amplitude. The gray blob represents the spin invariant for the coupled quark pair in the effective Lagrangian, Eq. (1). The black circle attached to the quark line represents the action of the electromagnetic current operator.

resented by four three-dimensional two-loop diagrams in Fig. 1 [27]. The diagrams embody the antisymmetrization of the quark state in the wave function.

The matrix elements of the electromagnetic current are calculated considering only the process on quark-3, due to the symmetrization of the microscopic matrix element after the factorization of the color degree of freedom. Therefore, the microscopic operator of the nucleon electromagnetic current is the sum of each amplitude represented by the diagrams (1a) to (1d) in Fig. 1, as

$$J^+_N(Q^2) = J^+_{aN}(Q^2) + 4J^+_{bN}(Q^2) + 2J^+_{cN}(Q^2) + 2J^+_{dN}(Q^2), \tag{7}$$

with the appropriate statistical factors from the identity of quarks 1 and 2. Another factor of 2 is multiplied to J^+_{bN} due to the exchange between the quark pairs in the initial and final state nucleons, where the exchanged diagrams give the same matrix elements as a consequence of time reversal and parity transformation properties. The explicit expressions

and derivations made in [27] are also summarized in Appendix A.

In this work, the effective Lagrangian, Eq. (1), is a scalar coupling that corresponds to the spin-coupling coefficients in which the Melosh rotations of the quark spin have the arguments defined by the kinematical momentum of the quarks in pair, and in the nucleon rest frame constrained by the total momentum [63, 64], while in the Bakamjian-Thomas construction the argument of the Melosh rotations are defined in the rest frame of three free particles (constituent quarks).

The model of the nucleon adopted here assumes the dominance of the valence component. The results are strongly constrained, and the general features found in our calculations are rather independent of the detailed shape of the wave function, but depend on the momentum scales in Eq. (2). In the numerical evaluation of the form factors, we use a constituent quark mass value of $m_q = 0.22$ GeV [27, 51]. This value was also used in the study of pion properties in vacuum as well as in medium [23–26] using a light-front constituent quark model. In addition, the model has three fitting parameters, the momentum scales β and β_1, and the relative weight λ, or M_H (see Eqs. (2) and (3)). We have selected two parameter sets for the present two-scale model, which will be denoted by "set I" and "set II", reproducing the proton magnetic moment (μ_p), and neutron magnetic moment (μ_n), respectively, as well as the zero of proton electric to magnetic form factor ratio Q_0^2 for $\mu_p G_{Ep}(Q_0^2)/G_{Mp}(Q_0^2) = 0$, or $G_{Ep}(Q_0^2) = 0$. In table I we summarize the model parameters for the set I and set II, some nucleon static observables calculated, and the zero, Q_0^2, of $G_{Ep}(Q_0^2) = 0$.

We remind that, a single-scale nucleon light-front wave function, Gaussian or power-law, with the proton or neutron magnetic moment fitted, is known to give a reasonable proton charge radius, due to the strong correlation between these observables [27, 47, 55]. However, the zero of $G_{Ep}(Q^2)$, Q_0^2, appears at too small values in the range 3-4 GeV^2. When we attempt to fit Q_0^2 to the values around or larger than 8 GeV^2 by increasing the momentum scale in the Gaussian and power-law nucleon wave functions of the one-scale model, we find too small proton size, and consequently bad magnetic moment values. Thus, the facts leave us no room for improving the one-scale-based models. However, by introducing a two-scale, namely, power-law high-momentum component in the wave function with the scalar coupling, we are able to get a reasonable description of both the nucleon static observables and the zero of $G_{Ep}(Q^2)$, as shown in table I. The scalar coupling provides the best agreement with the neutron charge radius, when the neutron magnetic moment is fitted [27]. Note that,

TABLE I: Nucleon electromagnetic static observables and the zero of $G_{Ep}(Q_0^2) = 0$, Q_0^2, for the two-scale models with the two sets of the parameters, set I and set II. The momentum-scale parameters, β, β_1 and M_H in Eqs. (2) and (3), are given in the second, third and fourth columns, respectively. The proton [neutron] magnetic moment μ_p [μ_n] (in nuclear magneton) and proton [neutron] mean square charge radius r_p^2 [r_n^2], are given in fifth [seventh] and sixth [eighth] columns respectively. The zero, Q_0^2 value for $G_{Ep}(Q_0^2) = 0$, is given in the last column. See table II, for the experimental values.

	β (GeV)	β_1 (GeV)	M_H (GeV)	μ_p	r_p (fm)	μ_n	r_n^2 (fm)^2	Q_0^2 GeV^2
Set I	0.676	5.72	4.79	2.74	0.80	-1.52	-0.07	8.31
Set II	0.396	10.56	5.92	3.05	0.94	-1.88	-0.06	15.1

TABLE II: Experimental values for some nucleon observables.

Ref.	μ_p [μ_N]	$\sqrt{r_p^2}$ [fm]	μ_n [μ_N]	r_n^2 [fm^2]
[65, 66]	2.792847351 ± 10^{-9}	0.8751 ± 0.000061		
[67]		0.879 ± 0.0008		
[65]			-1.9130427 ± 5.10^{-7}	-0.1161 ± 0.0022

the high-momentum scale $M_H \sim 7.6$ GeV, should be understood as a reference value, and we point out that we cannot exclude completely the lower values for M_H, as one can see the parameterization, $M_H = 4.79$ GeV. Using these two parameter sets, set I and set II, we study the nucleon electromagnetic form factors in vacuum and in a nuclear medium.

In Fig. 2 we show the results for the proton electric (upper panel) and magnetic (lower panel) form factors in vacuum, for the two sets of the parameters. The experimental data are well described by the parameter set II.

Next, we show in Fig. 3 the form factor ratio, $\mu_p G_{Ep}(Q^2)/G_{Mp}(Q^2)$, calculated with the two parameter sets, the same as those in Fig. 2. Reasonable and better agreement with the data [30, 32–37] is achieved for the parameter set II. The values of the zero for $G_{Ep}(Q^2)$, Q_0^2, are given in table I for both the set I and set II. The zero of the form factor ratio in vacuum by the set II, $Q_0^2 \simeq 15$ GeV^2, is one of the main results of this study. On the other hand, based

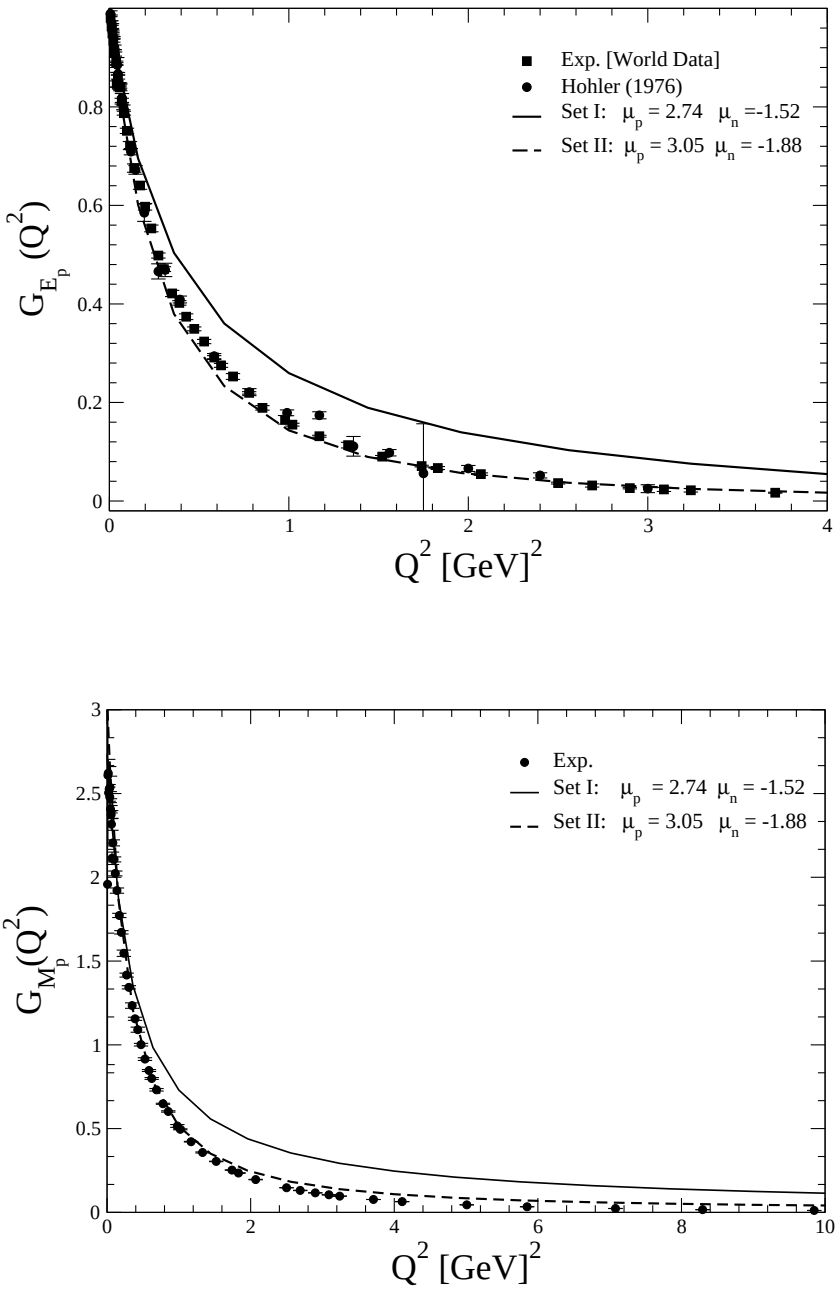

FIG. 2: Proton electric (upper panel) and magnetic (lower panel) form factors calculated with the two-scale model, with the two parameter sets, set I (solid line), and set II (dashed line). (See also table I.) Experimental data are from Refs. [30, 32–37, 71, 72].

on the nucleon Bethe-Salpeter amplitude and vector meson dominance model, Refs. [68, 69] report $Q_0^2 \simeq 9$ GeV^2. In addition, based on the covariant spectator quark model, Ref. [70] also obtained $Q_0^2 \simeq 9$ GeV^2 for $G_{Ep}(Q_0^2)/G_D(Q_0^2) = 0$, with $G_D(Q^2) = (1+Q^2/0.71\text{GeV}^2)^{-2}$.

We show in Fig. 4, the neutron electric (upper panel) and magnetic (lower panel) form

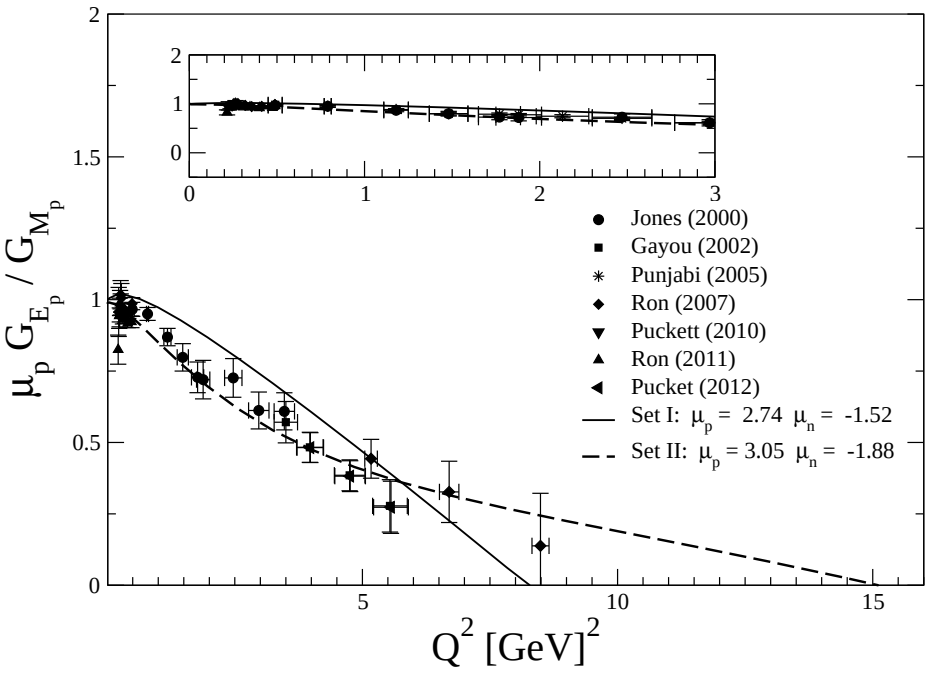

FIG. 3: Proton form factor ratio, $\mu_p G_{Ep}(Q^2)/G_{Mp}(Q^2)$, calculated with the two-scale model with the two parameter sets, set I and set II. Experimental data are from Refs. [30, 32–37] .

factors calculated in the two-scale model with the two sets of the parameters.

As one can see, the parameter set II describes better the data due to the strong sensitivity to $G_{En}(Q^2)$ [27]. Note that there is a zero in neutron magnetic form factor for the two-scale nucleon wave function in both parameter sets. The best fit for the experimental data of neutron magnetic form factor is achieved by the set II.

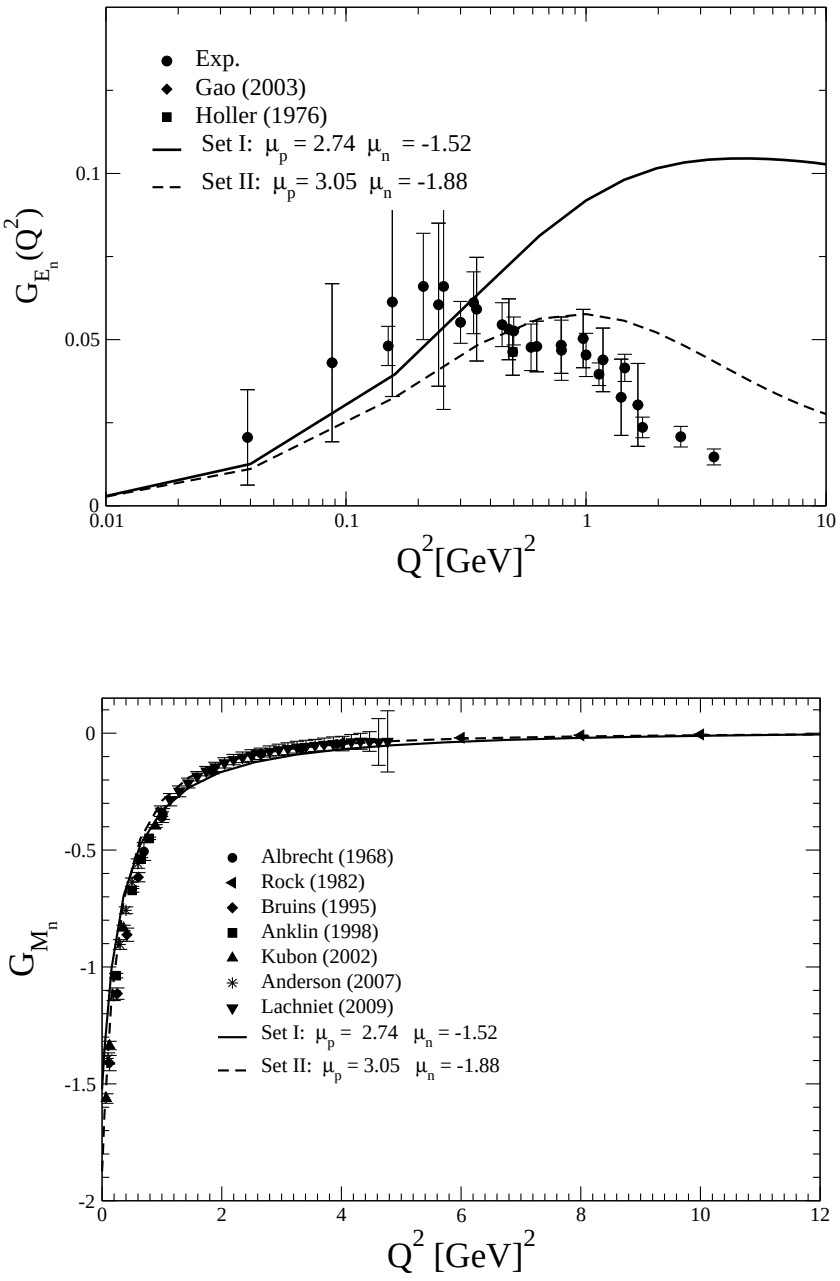

FIG. 4: Neutron electric (upper panel) and magnetic (lower panel) form factors calculated by the two-scale model with the two parameter sets. Experimental data are from [71, 72] for G_{E_n}, and from [74–80] for G_{M_n}.

III. QUARKS IN NUCLEAR MATTER: BRIEF REVIEW

In order to study the in-medium modifications of the nucleon electromagnetic form factors, we need a reasonable model of nuclear matter based on the quark degrees of freedom as well as the nucleon model in vacuum, since our interest is the nucleon internal structure

change in a nuclear medium.

As for the model of nuclear matter, we use the quark-meson coupling (QMC) model, which has been successfully applied for the studies of hadronic properties in nuclear medium and finite nuclei [3, 73]. This model was already used for the study of the in-medium pion properties [23–25, 25, 26] combined with a light-front constituent quark model. Therefore, we can extend the study of pion properties in medium for the nucleon electromagnetic form factors in a similar manner. We first review the quark model description of nuclear matter via the QMC model, and present the of nuclear saturation properties, as well as the in-medium constituent light quark properties, the same input used in the study of pion properties in medium [23–26].

A. Quark model of nuclear matter: quark-meson coupling (QMC) model

The QMC model was introduced by Guichon [22] in 1988 using the MIT bag model, and also by Frederico *et al.* in 1989 [81] using a confining harmonic potential, to describe the properties of nuclear matter based on the quark degrees of freedom. In this study we use the model of Guichon with the MIT bag model. The model has been successfully applied for various studies of finite (hyper)nuclei [73] as well as the hadron properties in a nuclear medium (see Ref. [3] for a review). In the model the medium effects arise through the self-consistent coupling of the isoscalar-Lorentz-scalar (σ), isoscalar-Lorentz-vector (ω) and isovector-Lorentz-vector (ρ) meson mean fields directly to the confined light-flavor u and d valence quarks — rather than to the nucleons. As a result the internal structure of the bound nucleon is modified by the surrounding nuclear medium with respect to the free nucleon.

The effective Lagrangian density of the QMC model for a uniform, spin-saturated, and isospin-symmetric infinite nuclear matter at the hadronic level is given by [3, 22, 73],

$$\mathcal{L} = \bar{\psi}[i\gamma\cdot\partial - m_N^*(\hat{\sigma}) - g_\omega\hat{\omega}^\mu\gamma_\mu]\psi + \mathcal{L}_{\rm meson}, \tag{8}$$

where ψ, $\hat{\sigma}$ and $\hat{\omega}$ are respectively the nucleon, Lorentz-scalar-isoscalar σ, and Lorentz-vector-isoscalar ω field operators, with

$$m_N^*(\hat{\sigma}) \equiv m_N - g_\sigma(\hat{\sigma})\hat{\sigma}, \tag{9}$$

which defines the σ-field dependent coupling constant, $g_\sigma(\hat{\sigma})$, while g_ω is the nucleon-ω coupling constant. All the important effective nuclear many-body dynamics including 3-

TABLE III: Coupling constants, the parameter Z_N, bag constant B (in $B^{1/4}$), and calculated properties for symmetric nuclear matter at normal nuclear matter density $\rho_0 = 0.15$ fm^{-3}, for $m_q = 5$ and 220 MeV (the latter values is used in this study and Refs. [23–26]). The effective nucleon mass, m_N^*, and the nuclear incompressibility, K, are quoted in MeV (the free nucleon bag radius input is $R_N = 0.8$ fm, the standard value in the QMC model [3]).

m_q(MeV)	$g_\sigma^2/4\pi$	$g_\omega^2/4\pi$	m_N^*	K	Z_N	$B^{1/4}$(MeV)
5	5.39	5.30	754.6	279.3	3.295	170
220	6.40	7.57	698.6	320.9	4.327	148

body nucleon force modeled at the quark level, can be regarded as effectively condensed in $g_\sigma(\hat{\sigma})$. Solving the Dirac equations for the up and down quarks in the nuclear medium with the same mean fields (mean values) σ and ω which act on the bound nucleon self-consistently based on Eq. (8), we obtain the effective σ-dependent coupling $g_\sigma(\sigma)$ at the nucleon level [3, 22, 73]. The free meson Lagrangian density is given by,

$$\mathcal{L}_{\rm meson} = \frac{1}{2}(\partial_\mu\hat{\sigma}\partial^\mu\hat{\sigma} - m_\sigma^2\hat{\sigma}^2) - \frac{1}{2}\partial_\mu\hat{\omega}_\nu(\partial^\mu\hat{\omega}^\nu - \partial^\nu\hat{\omega}^\mu) + \frac{1}{2}m_\omega^2\hat{\omega}^\mu\hat{\omega}_\mu \ , \tag{10}$$

where we have ignored the isospin-dependent Lorentz-vector-isovector ρ-meson field, since we consider isospin-symmetric nuclear matter within the Hartree mean-field approximation. In this case the mean value of the ρ-meson field becomes zero and there is no need to consider its possible contributions due to the ρ-Fock (exchange) terms.

In the following we work in the nuclear matter rest frame. For symmetric nuclear matter in the Hartree mean-field approximation, the nucleon Fermi momentum k_F (baryon density ρ) and the scalar density (ρ_s) associated with the σ-mean field can be related as,

$$\rho = \frac{4}{(2\pi)^3}\int d^3k\ \theta(k_F - |\vec{k}|) = \frac{2k_F^3}{3\pi^2}, \tag{11}$$

$$\rho_s = \frac{4}{(2\pi)^3}\int d^3k\ \theta(k_F - |\vec{k}|)\frac{m_N^*(\sigma)}{\sqrt{m_N^{*2}(\sigma) + \vec{k}^2}}, \tag{12}$$

where $m_N^*(\sigma)$ is the constant value of the effective nucleon mass at a given density, and is calculated in the standard QMC model [3, 22, 73]. The Dirac equations for the up (u) and down (d) quarks in symmetric nuclear matter are solved self-consistently with the same σ

and ω mean-field potentials acting for the nucleon. We restrict ourselves hereafter the flavor SU(2), the light-quark sector (as well as for the proton and neutron). The Dirac equations for the quarks and antiquarks ($q = u$ or d, quarks) in the bag of hadron h in nuclear matter at the position $x = (t, \vec{r})$ ($|\vec{r}| \leq$ bag radius) are given by [3],

$$\left[i\gamma \cdot \partial_x - (m_q - V_\sigma^q) \mp \gamma^0 \left(V_\omega^q + \frac{1}{2} V_\rho^q \right) \right] \begin{pmatrix} \psi_u(x) \\ \psi_{\bar{u}}(x) \end{pmatrix} = 0, \tag{13}$$

$$\left[i\gamma \cdot \partial_x - (m_q - V_\sigma^q) \mp \gamma^0 \left(V_\omega^q - \frac{1}{2} V_\rho^q \right) \right] \begin{pmatrix} \psi_d(x) \\ \psi_{\bar{d}}(x) \end{pmatrix} = 0, \tag{14}$$

where we have neglected the Coulomb force as usual, since the nuclear matter properties are due to the strong interaction, and we assume SU(2) symmetry for the light quarks, $m_q = m_u = m_d$, and define $m_q^* \equiv m_q - V_\sigma^q = m_u^* = m_d^*$. In symmetric nuclear matter, the isospin dependent ρ-meson mean field in Hartree approximation yields $V_\rho^q = 0$ in Eqs. (13) and (14), as mentioned already, so we ignore it hereafter. The constant mean-field potentials in nuclear matter are defined by, $V_\sigma^q \equiv g_\sigma^q \sigma = g_\sigma^q < \sigma >$ and $V_\omega^q \equiv g_\omega^q \omega = g_\omega^q \, \delta^{\mu,0} < \omega^\mu >$, with g_σ^q and g_ω^q being the corresponding quark-meson coupling constants, and the quantities inside the brackets stand for taking expectation values by the nuclear matter ground state [3]. Note that, since the velocity averages to zero in the rest frame of nuclear matter, the mean vector source due to the quark fields as well, $< \bar{\psi}_q \vec{\gamma} \psi_q >= 0$. Thus we may just keep the term proportional to γ^0 in Eqs. (13) and (14).

The normalized, static solution for the ground state quarks or antiquarks with flavor f in the hadron h composed of light quarks, may be written, $\psi_f(x) = N_f e^{-i\epsilon_f t/R_h^*} \psi_f(\vec{r})$, where N_f and $\psi_f(\vec{r})$ are the normalization factor and corresponding spin and spatial part of the wave function. The bag radius in medium for a hadron h, R_h^*, is determined through the stability condition for the mass of the hadron against the variation of the bag radius [3]. The eigenenergies in units of $1/R_h^*$ are given by,

$$\begin{pmatrix} \epsilon_u \\ \epsilon_{\bar{u}} \end{pmatrix} = \Omega_q^* \pm R_h^* \left(V_\omega^q + \frac{1}{2} V_\rho^q \right), \quad \begin{pmatrix} \epsilon_d \\ \epsilon_{\bar{d}} \end{pmatrix} = \Omega_q^* \pm R_h^* \left(V_\omega^q - \frac{1}{2} V_\rho^q \right). \tag{15}$$

The hadron masses in a nuclear medium m_h^* (free mass m_h), are calculated by

$$m_h^* = \sum_{j=q,\bar{q}} \frac{n_j \Omega_j^* - z_h}{R_h^*} + \frac{4}{3} \pi R_h^{*3} B, \quad \left. \frac{\partial m_h^*}{\partial R_h} \right|_{R_h = R_h^*} = 0, \tag{16}$$

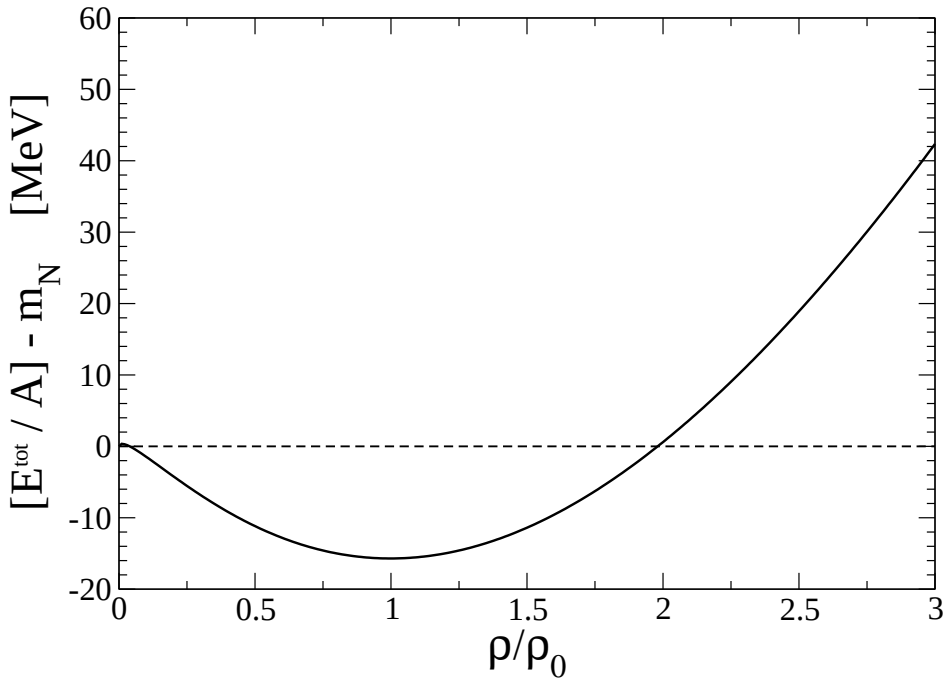

FIG. 5: Negative of the binding energy per nucleon ($E^{\rm tot}/A - m_N$) for symmetric nuclear matter calculated with the vacuum up and down quark mass, $m_q = 220$ MeV, taken from Ref. [23–26]. At the saturation point $\rho_0 = 0.15$ fm^{-3}, the value is fitted to -15.7 MeV. (See Ref. [3] for the $m_q = 5$ MeV case, denoted in there as QMC-I.)

where $\Omega_q^* = \Omega_{\bar{q}}^* = [x_q^2 + (R_h^* m_q^*)^2]^{1/2}$, with $m_q^* = m_q - g_\sigma^q \sigma$, and x_q being the lowest bag eigenfrequencies. $n_q(n_{\bar{q}})$ is the quark (antiquark) numbers for the quark flavors q. The MIT bag quantities, z_h, B, x_q, and m_q are the parameters for the sum of the c.m. and gluon fluctuation effects, bag constant, lowest eigenvalues for the quarks q, and the corresponding current quark masses. z_N and B (z_h) are fixed by fitting the nucleon (the hadron) mass in free space. (See table III for the nucleon case.)

For the nucleon $h = N$ in the above, the lowest, positive energy bag eigenfunction is given by

$$q(t,\vec{r}) = \frac{\mathcal{N}}{\sqrt{4\pi}} e^{-i\epsilon_q t/R_N^*} \begin{pmatrix} j_0(xr/R_N^*) \\ i\beta_q \vec{\sigma}\cdot\hat{r} j_1(xr/R_N^*) \end{pmatrix} \theta(R_N^* - r)\chi_m, \tag{17}$$

with $r = |\vec{r}|$ and χ_m the spin function and

$$\Omega_q^* = \sqrt{x^2 + (m_q^* R_N^*)^2}, \quad \beta_q = \sqrt{\frac{\Omega_q^* - m_q^* R_N^*}{\Omega_q^* + m_q^* R_N^*}}, \tag{18}$$

$$\mathcal{N}^{-2} = 2R_N^{*3} j_0^2(x)[\Omega_q^*(\Omega_q^* - 1) + m_q^* R_N^*/2]/x^2, \tag{19}$$

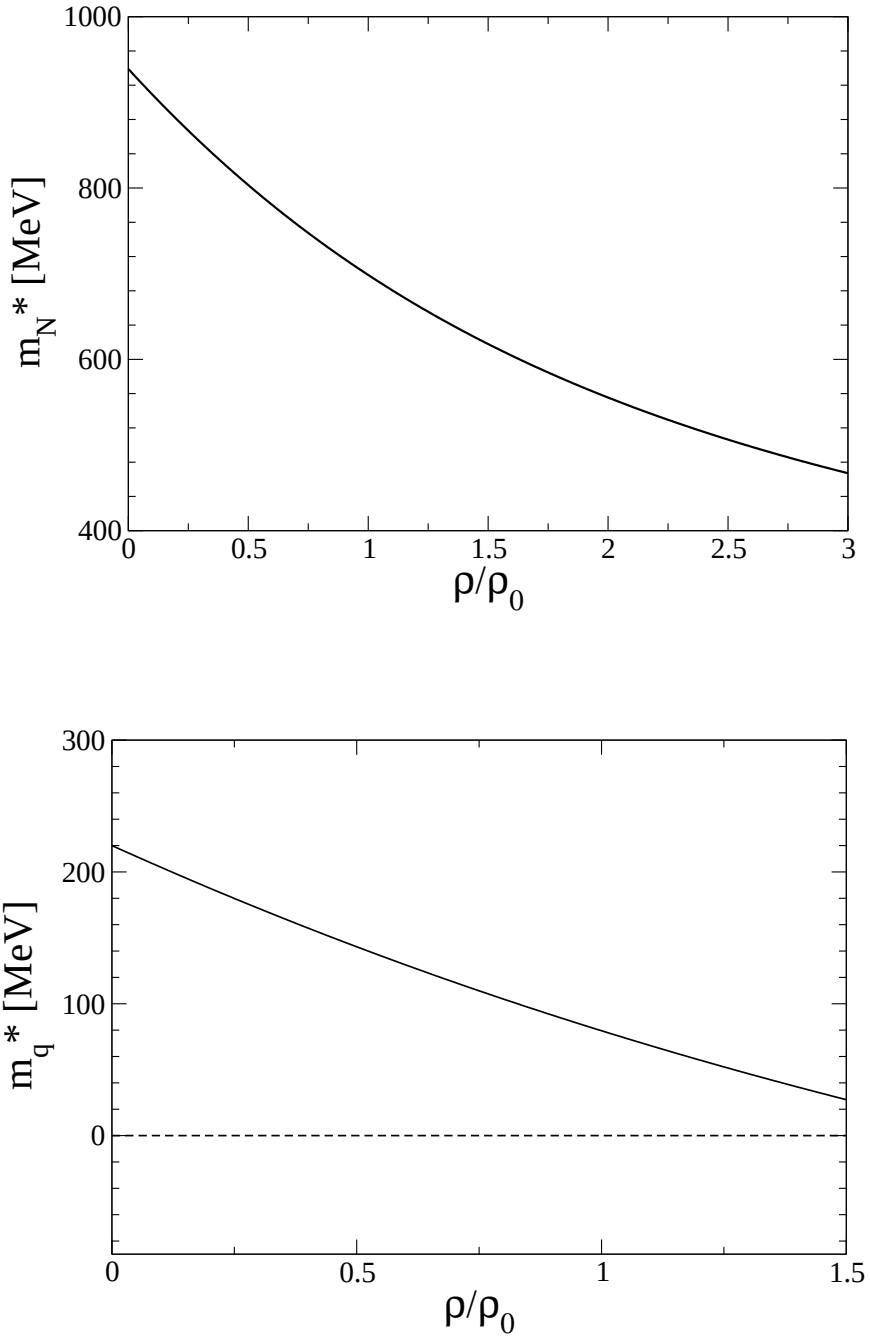

FIG. 6: Nucleon and constituent quark effective masses, respectively m_N^* (upper panel), and m_q^* (lower panel) where $m_q^* \equiv m_u^* = m_d^*$, in symmetric nuclear matter taken from Refs. [23–26]. See also caption of Fig. 5.

where x is the eigenvalue for the lowest mode, which satisfies the boundary condition at the bag surface, $j_0(x) = \beta_q j_1(x)$ with $j_{0,1}$ are the spherical Bessel functions.

The same meson mean fields σ and ω for the quarks and nucleons satisfy the following equations at the nucleon level self-consistently:

$$\omega = \frac{g_\omega \rho}{m_\omega^2}, \tag{20}$$

$$\sigma = \frac{g_\sigma}{m_\sigma^2} C_N(\sigma) \frac{4}{(2\pi)^3} \int d^3k \; \theta(k_F - |\vec{k}|) \frac{m_N^*(\sigma)}{\sqrt{m_N^{*2}(\sigma) + \vec{k}^2}} = \frac{g_\sigma}{m_\sigma^2} C_N(\sigma) \rho_s, \tag{21}$$

$$C_N(\sigma) = \frac{-1}{g_\sigma(\sigma = 0)} \left[\frac{\partial m_N^*(\sigma)}{\partial \sigma} \right], \tag{22}$$

where $C_N(\sigma)$ is the constant value of the scalar density ratio [3, 22, 73]. Because of the underlying quark structure of the nucleon used to calculate $M_N^*(\sigma)$ in the nuclear medium (see Eq. (16) with $h = N$), $C_N(\sigma)$ gets nonlinear σ-dependence, whereas the usual point-like nucleon-based model yields unity, $C_N(\sigma) = 1$. It is this $C_N(\sigma)$ or $g_\sigma(\sigma)$ that gives a novel saturation mechanism in the QMC model, and contains the important dynamics which originates from the quark structure of the nucleon. Without an explicit introduction of the nonlinear couplings of the meson fields in the Lagrangian density at the nucleon and meson level, the standard QMC model yields the nuclear incompressibility of $K \simeq 280$ MeV with $m_q = 5$ MeV, which is in contrast to a naive version of quantum hadrodynamics (QHD) [82] (the point-like nucleon model of nuclear matter), results in the much larger value, $K \simeq 500$ MeV; the empirically extracted value falls in the range $K = 200 - 300$ MeV. (See Ref. [83] for the updated discussions on the incompressibility.)

Once the self-consistency equation for the σ, Eq. (21), has been solved, one can evaluate the total energy per nucleon:

$$E^{\rm tot}/A = \frac{4}{(2\pi)^3 \rho} \int d^3k \; \theta(k_F - |\vec{k}|) \sqrt{m_N^{*2}(\sigma) + \vec{k}^2} + \frac{m_\sigma^2 \sigma^2}{2\rho} + \frac{g_\omega^2 \rho}{2 m_\omega^2}. \tag{23}$$

We then determine the coupling constants, g_σ and g_ω, so as to fit the binding energy of 15.7 MeV at the saturation density $\rho_0 = 0.15$ fm^{-3} ($k_F^0 = 1.305$ fm^{-1}) for symmetric nuclear matter.

In the study of pion properties in medium [23–26] based on a light-front constituent quark model, the vacuum value of the light-quark constituent, $m_q = 220$ MeV was used and could reproduce well the electromagnetic form factor and decay constant in vacuum [38].

To be consistent and encouraged by the studies for the pion properties in a nuclear medium [23–26], we build the nuclear matter with the same light-quark constituent mass in vacuum. The corresponding coupling constants and some results for symmetric nuclear matter at the saturation density calculated with $m_q = 220$ MeV and the standard values of $m_\sigma = 550$ MeV and $m_\omega = 783$ MeV, are listed in Table III. For comparison, we also give the corresponding quantities calculated in the standard QMC model with a vacuum quark mass of $m_q = 5$ MeV (see Ref. [3] for details). Thus, we have obtained the in-medium properties of the light-constituent quarks in symmetric nuclear matter with the vacuum mass of $m_q = 220$ MeV. Namely, we obtain the density dependence of the effective mass (scalar potential) and vector potential. Using the obtained in-medium input, we study the nucleon electromagnetic form factors in symmetric nuclear matter.

In Figs. 5 and 6, we respectively show the results for the negative of the binding energy per nucleon ($E^{\rm tot}/A - m_N$), effective mass of the nucleon, m_N^*, and effective mass of the constituent up and down quarks, m_q^*, in symmetric nuclear matter.

As one can expect from the values of the incompressibility, $K = (279.3, 320.9)$ MeV for m_q $(5, 220)$ MeV, in Table III, the result for $E/A - m_N$ with $m_q = 220$ MeV shown in Fig. 5 varies slightly faster than that for the case of $m_q = 5$ MeV [3] as increasing nuclear density. As for the effective nucleon mass shown in Fig. 6 with $m_q = 220$ MeV, it also decreases faster than that for $m_q = 5$ MeV [3] as increasing nuclear density.

In next section we study the nucleon electromagnetic form factors in a nuclear medium using the in-medium constituent quark properties obtained so far.

IV. NUCLEON ELECTROMAGNETIC FORM FACTORS IN MEDIUM

In this section we present our main results, the nucleon electromagnetic form factors in symmetric nuclear matter, $G^*_{Ep}(Q^2), G^*_{Mp}(Q^2), G^*_{En}(Q^2), G^*_{Mn}(Q^2)$, the ratio, $\mu_p G^*_{Ep}(Q^2)/G^*_{Mp}(Q^2)$, and the double ratio, $R_p \equiv [G^*_{Ep}(Q^2)/G^*_{Mp}(Q^2)]/[G_{Ep}(Q^2)/G_{Mp}(Q^2)]$. Our interests in this section are, in-medium effects on the zero of $\mu_p G^*_{Ep}(Q^2)/G^*_{Mp}(Q^2)$, and the comparison with the JLab data for $[G^{^4\rm He}_{Ep}(Q^2)/G^{^4\rm He}_{Mp}(Q^2)]/[G^{^1\rm H}_{Ep}(Q^2)/G^{^1\rm H}_{Mp}(Q^2)]$. The nuclear densities $\rho = 0.3\rho_0$ and $0.4\rho_0$ studied in this section (except for the set II in Fig. 10), are chosen so that to give a trend of medium effects, based on a rough estimate made for the proton electromagnetic double ratio by the set I to be shown later in Fig. 10.

First, we show in Fig. 7 in-medium proton electric $G^*_{Ep}(Q^2)$ (upper panel) and magnetic G^*_{Mp} (lower panel) form factors in the two-scale model with the two parameter sets, set I and set II, for nuclear densities of $\rho = 0.3\rho_0$ and $0.4\rho_0$ ($\rho_0 = 0.15$ fm^{-3}), together with those in vacuum to make easier to see the medium effects. For $G^*_{Ep}(Q^2)$, the falloff becomes faster as increasing nuclear density than that in vacuum. This means that the proton charge radius increases in nuclear matter. The fast falloff of the electric electric form factor was also found in Refs. [84, 85]. From this behavior, we can expect the zero of $G^*_{Ep}(Q^2)$ in medium shifts to a smaller Q^2 value.

As for $G^*_{Mp}(Q^2)$, the in-medium proton magnetic moment $\mu^*_p = G^*_p(0)$ is enhanced than that in vacuum as increasing nuclear density. This enhancement is also, observed in Refs. [84, 85]. However, as increasing Q^2, the falloff of the in medium one, $G^*_{Mp}(Q^2)$, becomes faster than that in vacuum.

Based on the results shown in Fig. 7, we show in Fig. 8 the result for $\mu^*_p G^*_{Ep}(Q^2)/G^*_{Mp}(Q^2)$, in symmetric nuclear matter as well as in vacuum. This is our second main results and the other prediction of this article. For each parameter set, the value of Q^2_0, to cross the zero $\mu^*_p G^*_{Ep}(Q^2_0)/G^*_{Mp}(Q^2_0) = 0$, becomes smaller than that in vacuum. This reflects that the in-medium falloff of $G^*_{Ep}(Q^2)$ becomes faster than that in vacuum as already mentioned. Thus, it is very interesting to pursue experiment to measure the proton electromagnetic form factor ratio of the bound proton, to check if this Q^2 reduction of crossing the zero can be observed, although such experiment would be challenging. However, we would like to emphasize this is a very interesting prediction of the present study. We believe that this is the first time prediction that made with an explicit calculation.

Next, in Fig. 9 we show the in-medium neutron electric $G^*_{En}(Q^2)$ (upper panel), and magnetic $G^*_{Mn}(Q^2)$ (lower panel) form factors. For both parameter sates, set I and set II, $G^*_{En}(Q^2)$ is suppressed than that in vacuum as increasing Q^2, while very small region of Q^2, $G^*_{En}(Q^2)$ is enhanced than that in vacuum.

As for the magnetic form factor, the absolute values in medium, $|G^*_{Mn}(Q^2)|$, becomes smaller than that in vacuum for whole region of Q^2 studied. This means that the "negative falloff" becomes faster, or Q^2 dependence becomes more sensitive, the same as that for the proton case.

Finally, in Fig. 10, we show our third main result of this article, the result of the proton form factor double ratio, $[G^*_{Ep}(Q^2)/G^*_{Mp}(Q^2)]/[G_{Ep}(Q^2)/G_{Mp}(Q^2)]$ in symmetric nuclear

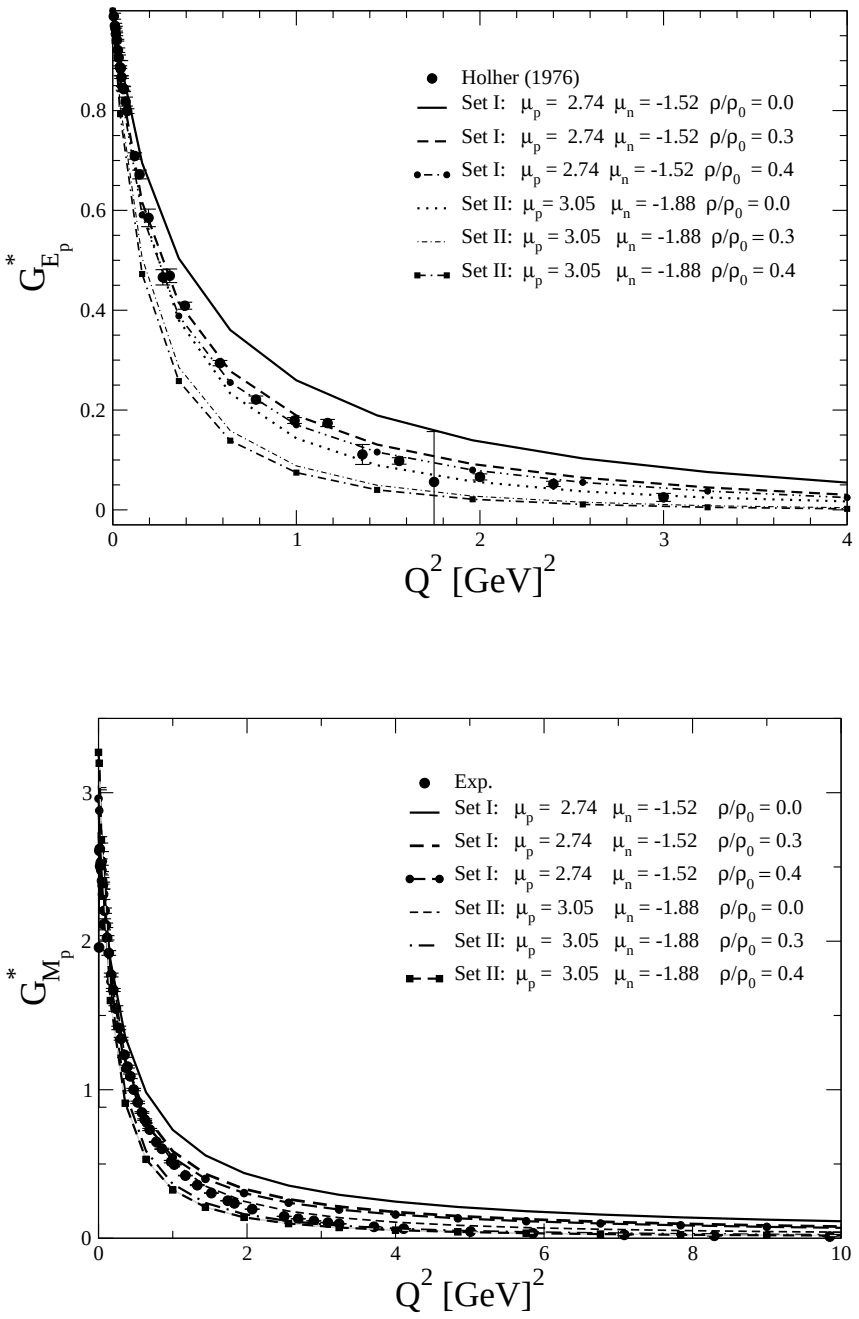

FIG. 7: Proton electric $G^*_{Ep}(Q^2)$ (upper panel), and magnetic form $G^*_{Mp}(Q^2)$ (lower panel) form factors calculated in the two-scale model with the two parameter sets, set I and set II, for nuclear densities $\rho = 0.3\rho_0$ and $0.4\rho_0$ with $\rho_0 = 0.15$ fm^{-3}, together with those in vacuum. (See also table I.) Experimental word data are from [86–92]

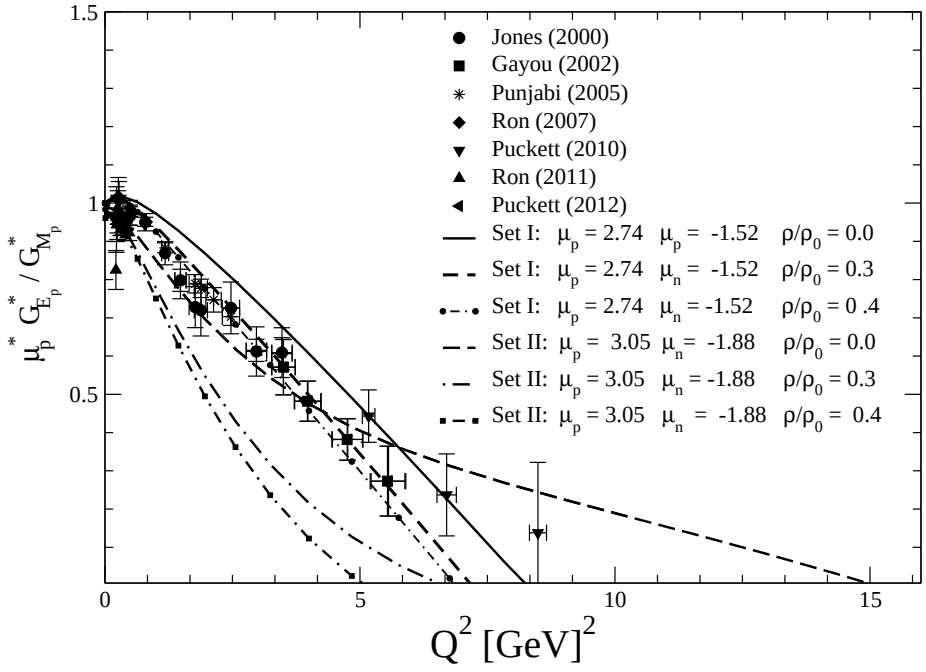

FIG. 8: $\mu_p^* G_{Ep}^*(Q^2)/G_{Mp}^*(Q^2)$ calculated with the two-scale model with the two parameter sets, for the nuclear densities $\rho = 0.3\rho_0$ and $0.4\rho_0$.

matter in the two-scale model with the set I and set II, compared with the JLab data. The good description of the JLab data is obtained by the both parameter sets, set I and set II, by the different nuclear densities. Namely, for the set I with the nuclear density $0.3\rho_0$, and for the set II the nuclear density $0.15\rho_0$, the JLab data are well described. Recall that the zero of $\mu_p G_{Ep}(Q^2)/G_{Mp}(Q^2)$ and the nucleon electromagnetic form factors in vacuum, can be better described with the set II.

We have also calculated the double ratio using the one-scale model that fits experimental proton magnetic moment better, for the nuclear densities $0.3\rho_0$ and $0.4\rho_0$ as examples, but it gives a very poor description of the data, and thus we do not show the results. For a comparison between the one-scale and two-scale models made in the past, see Ref. [64].

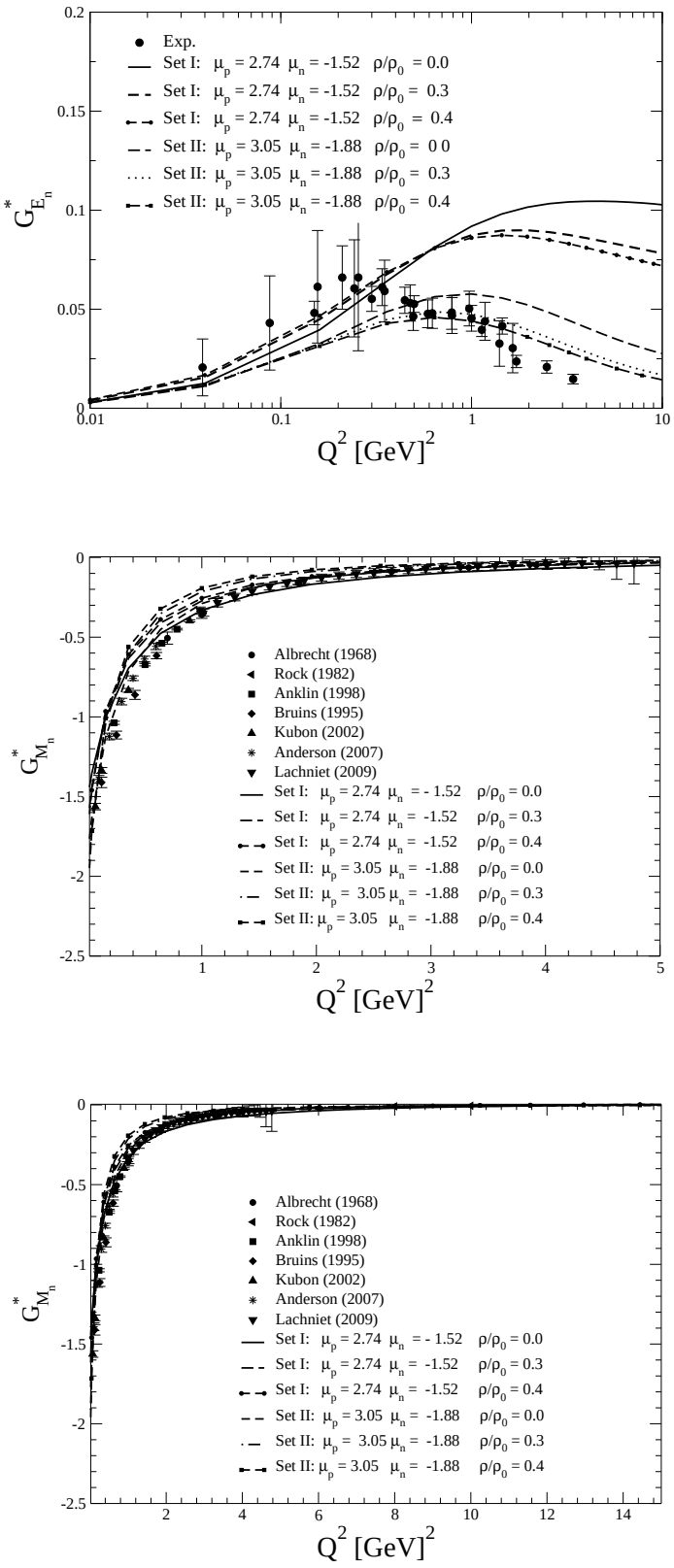

FIG. 9: Neutron electric $G^*_{En}(Q^2)$ (upper panel) and magnetic $G^*_{Mn}(Q^2)$ (middle and bottom panels) form factors in medium, obtained by the two-scale model with the two sets of parameters, for $\rho = 0.3\rho_0$ and $0.4\rho_0$. Those in vacuum are shown for references.

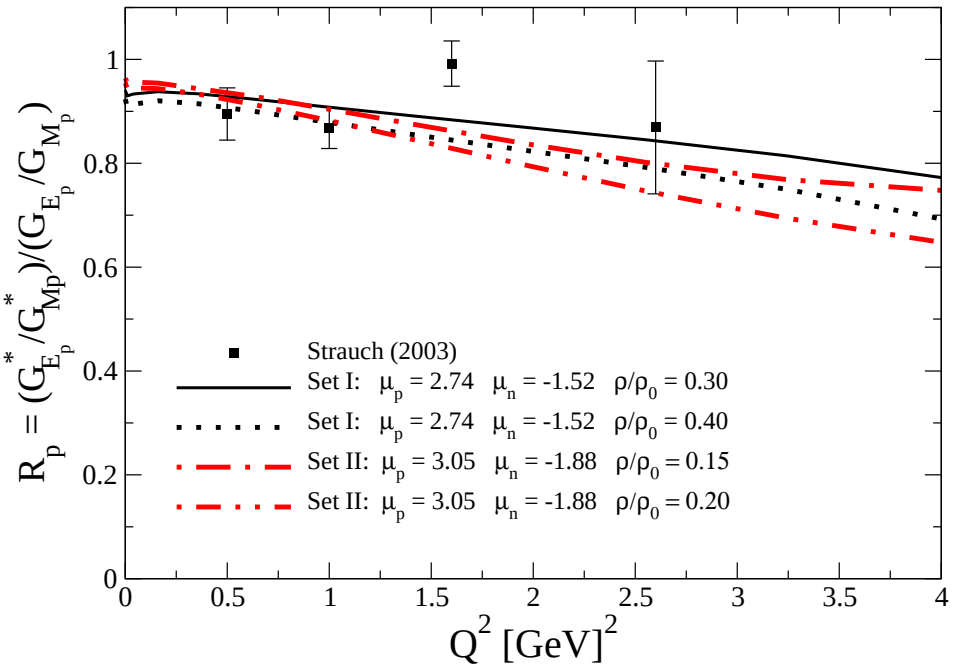

FIG. 10: Proton electromagnetic form factor double ratio in symmetric nuclear matter, $R_p \equiv [G^*_{Ep}(Q^2)/G^*_{Mp}(Q^2)]/[G_{Ep}(Q^2)/G_{Mp}(Q^2)]$, calculated by the two-scale model with the two parameter sets, by the set I for nuclear densities $0.30\rho_0$ and $0.40\rho_0$, and by the set II for nuclear densities $0.15\rho_0$ and $0.20\rho_0$, compared with the JLab data extracted for $[G^{^4\mathrm{He}}_{Ep}(Q^2)/G^{^4\mathrm{He}}_{Mp}(Q^2)]/[G^{^1\mathrm{H}}_{Ep}(Q^2)/G^{^1\mathrm{H}}_{Mp}(Q^2)]$. The experimental data are taken from Ref. [14].

V. SUMMARY AND DISCUSSIONS

We have studied the nucleon electromagnetic form factors in medium as well as in vacuum, using the light-front motivated quark-spin coupling model with the one- and two-scale models of the nucleon wave function. The in-medium input for the light-constituent quark properties is calculated by the quark-meson coupling model, which has proven to be successful in describing the hadron properties in medium, as well as the properties of finite nuclei based on the quark degrees of freedom.

We have found that the two-scale nucleon wave function models describe well the nucleon electromagnetic form factors in vacuum. Our first prediction is that the zero of the proton electromagnetic form factor ratio (the zero of the proton electric form factor) in vacuum, to be about 15 GeV^2 based on our results including the new experimental data .

Based on the two-scale model with the two parameter sets which can reasonably repro-

duce the proton and neutron magnetic moments, we have studied the zero of the proton electromagnetic form factor ratio in medium. By the results, our second prediction of this study is that, the zero of the bound proton, or proton in finite nuclear density, shifts to a smaller Q^2 value than that in vacuum as nuclear density increases.

Using the same two-scale model with the same parameter sets, we have calculated the proton electromagnetic form factor double ratio, which were extracted in JLab experiments. The model with the parameter set I for nuclear density $0.3\rho_0$, and the parameter set II for nuclear density $0.15\rho_0$, are both able to describe well the JLab data. The results suggest that the description of the bound proton, or the in-medium electromagnetic form factor double ratio data, may be explained based on the internal structure change of the bound proton in a nuclear medium.

For the future prospects, we can also study the nucleon axial-vector form factor in nuclear medium with the same model. Furthermore, we plan to extend the model to study the octet baryon electromagnetic and axial-vector form factors in vacuum, as well as in a nuclear medium.

Acknowledgement

This work was partly supported by the Fundação de Amparo à Pesquisa do Estado de São Paulo (FAPESP), Nos. 2015/16295-5 (J.P.B.C.M.), and 2015/17234-0 (K.T.), and Conselho Nacional de Desenvolvimento Científico e Tecnológico (CNPq), Nos. 401322/2014-9, 308025/2015-6 (J.P.B.C.M.), and 400826/2014-3, 308088/2015-8 (K.T.) of Brazil.

APPENDIX A: MATRIX ELEMENTS OF THE MICROSCOPIC CURRENT

The derivation of the matrix elements of the microscopic nucleon current operator composed by $J^+_{\beta N}$, $\beta = a, b, c, d$ of Eq. (7) in terms of the valence nucleon wave function follows closely Refs. [27]. They are represented by the Feynman diagrams in Fig. 1. The blobs in the figure represent the color anti-triplet coupling of a pair of quark fields in scalar-isocalar ($\epsilon^{lmn}\overline{\Psi}_{(l)} i\tau_2\gamma_5 \Psi^C_{(m)}$) from the effective Lagrangian of Eq. (1).

The integrations over the minus-component of the momentum are performed to eliminate the relative light-front time in the intermediate state propagations [58]. This procedure allows to introduce the momentum component of the valence light-front wave function in

the computation of form factors (see Ref. [59]).

The nucleon electromagnetic current J_N^+ derived from the effective Lagrangian has contribution from each photo-absorption amplitude given by the Feynman two-loop triangle diagrams of Figs. 1a to 1d. The photon is absorbed by quark-3:

$$\begin{aligned}\langle s'|J_{aN}^+(q^2)|s\rangle &= -m_N^2\langle N|\hat{Q}_q|N\rangle \mathrm{Tr}[i\tau_2(-i)\tau_2]\int\frac{d^4k_1d^4k_2}{(2\pi)^8}\Lambda(k_i,p')\Lambda(k_i,p)\bar{u}(p',s')\\ &\times S(k_3')\gamma^+S(k_3)u(p,s)\mathrm{Tr}\left[S(k_2)\gamma^5S_c(k_1)\gamma^5\right]\ , \end{aligned}\tag{A1}$$

with $S(p)=\dfrac{1}{\not{p}-m+i\epsilon}$, and $S_c(p)=\left[\gamma^0\gamma^2\dfrac{1}{\not{p}-m+i\epsilon}\gamma^0\gamma^2\right]^T$ with T denoting transposition. The four-momentum of the virtual quark-3 after the photo-absorption process is $k_3'=k_3+q$. The matrix element of the quark charge operator in isospin space is $\langle N|\hat{Q}_q|N\rangle$. The function $\Lambda(k_i,p)$ is chosen to introduce the momentum part of the three-quark light-front wave function, after the integrations over k^-. The contribution to the electromagnetic current represented by Fig. 1b is given by:

$$\begin{aligned}\langle s'|J_{bN}^+(q^2)|s\rangle &= -m_N^2\langle N|\hat{Q}_q|N\rangle\int\frac{d^4k_1d^4k_2}{(2\pi)^8}\Lambda(k_i,p')\Lambda(k_i,p)\bar{u}(p',s')S(k_3')\gamma^+S(k_3)\\ &\times\gamma^5S_c(k_1)\gamma^5S(k_2)u(p,s)\ . \end{aligned}\tag{A2}$$

While the contribution to the electromagnetic current represented by Fig. 1c is given by:

$$\begin{aligned}\langle s'|J_{cN}^+(q^2)|s\rangle &= m_N^2\langle N|\tau_2\hat{Q}_q\tau_2|N\rangle\int\frac{d^4k_1d^4k_2}{(2\pi)^8}\Lambda(k_i,p')\Lambda(k_i,p)\bar{u}(p',s')S(k_1)\\ &\times\gamma^5S_c(k_3)\gamma^+S_c(k_3')\gamma^5S(k_2)u(p,s)\ . \end{aligned}\tag{A3}$$

Finally, the contribution to the electromagnetic current represented by Fig. 1d is given by:

$$\begin{aligned}\langle s'|J_{dN}^+(q^2)|s\rangle &= -m_N^2\mathrm{Tr}[\hat{Q}_q]\int\frac{d^4k_1d^4k_2}{(2\pi)^8}\Lambda(k_i,p')\Lambda(k_i,p)\bar{u}(p',s')S(k_2)u(p,s)\\ &\times\mathrm{Tr}\left[\gamma^5S(k_3')\gamma^+S(k_3)\gamma^5S_c(k_1)\right]\ . \end{aligned}\tag{A4}$$

The light-front coordinates are defined as $k^+=k^0+k^3$, $k^-=k^0-k^3$, $\vec{k}_\perp=(k^1,k^2)$. In each term of the nucleon current, from J_{aN}^+ to J_{dN}^+, the Cauchy integrations over k_1^- and k_2^- are performed. That means the on-mass-shell pole of the Feynman propagators for the spectator particles 1 and 2 of the photon absorption process are taken into account. In the Breit-frame with $q^+=0$, there is a maximal suppression of light-front Z-diagrams in J^+ [59, 60]. Thus the components of the momentum k_1^+ and k_2^+ are bounded such that

$0 < k_1^+ < p^+$ and $0 < k_2^+ < p^+ - k_1^+$. The four-dimensional integrations of Eqs. (A1) to (A4) are reduced to the three-dimensional ones on the null-plane.

After the integrations over the light-front energies the momentum part of the wave function is introduced into the microscopic matrix elements of the current by the substitution [27, 59]:

$$\frac{1}{2(2\pi)^3}\frac{\Lambda(k_i,p)}{m_N^2 - M_0^2} \to \Psi(M_0^2) \ . \tag{A5}$$

Further, the same momentum wave function is chosen all N-q coupling schemes for simplification. Note, that the mixed case, $\alpha = 1/2$ in Ref. [27] ($\alpha = 1$ is chosen for the present Lagrangian density of Eq. 1)), could have different momentum dependence for each spin coupling, however, we choose the same momentum functions just to keep contact to the Bakamjian-Thomas (BT) [93] approach.

The analytical integration of Eq. (A1) of the k^- components of the momenta yields:

$$\langle s'|J^+_{aN}(q^2)|s\rangle = 2p^{+2}m_N^2\langle N|\hat{Q}_q|N\rangle \int \frac{d^2k_{1\perp}dk_1^+ d^2k_{2\perp}dk_2^+}{k_1^+ k_2^+ k_3^{+\ 2}}\theta(p^+ - k_1^+)\theta(p^+ - k_1^+ - k_2^+)$$
$$\times \mathrm{Tr}\left[(\not{k}_2 + m)(\not{k}_1 + m)\right]\bar{u}(p',s')(\not{k}'_3 + m))\gamma^+(\not{k}_3 + m)u(p,s)\Psi(M_0'^2)\Psi(M_0^2) \ , \tag{A6}$$

where $k_1^2 = m^2$ and $k_2^2 = m^2$. The squared-mass of the free-three quarks is defined by:

$$M_0^2 = p^+(\frac{k_{1\perp}^2 + m^2}{k_1^+} + \frac{k_{2\perp}^2 + m^2}{k_2^+} + \frac{k_{3\perp}^2 + m^2}{k_3^+}) - p_\perp^2 \ , \tag{A7}$$

and $M_0'^2 = M_0^2(k_3 \to k'_3 \ , \vec{p}_\perp \to \vec{p}'_\perp)$.

The other terms of the nucleon current, as given by Eqs. (A2)-(A4) are also integrated over the k^- momentum components of particles 1 and 2 following the same steps used to obtain Eq. (A6) from Eq. (A1):

$$\langle s'|J^+_{bN}(q^2)|s\rangle = p^{+2}m_N^2\langle N|\hat{Q}_q|N\rangle \int \frac{d^2k_{1\perp}dk_1^+ d^2k_{2\perp}dk_2^+}{k_1^+ k_2^+ k_3^{+\ 2}}\theta(p^+ - k_1^+)\theta(p^+ - k_1^+ - k_2^+)$$
$$\times \bar{u}(p',s')(\not{k}'_3 + m)\gamma^+(\not{k}_3 + m)(\not{k}_1 + m)(\not{k}_2 + m)u(p,s)\Psi(M_0'^2)\Psi(M_0^2) \ , \tag{A8}$$

$$\langle s'|J^+_{cN}(q^2)|s\rangle = p^{+2}\langle N|\tau_2\hat{Q}_q\tau_2|N\rangle \int \frac{d^2k_{1\perp}dk_1^+ d^2k_{2\perp}dk_2^+}{k_1^+ k_2^+ k_3^{+\ 2}}\theta(p^+ - k_1^+)\theta(p^+ - k_1^+ - k_2^+)$$
$$\times \bar{u}(p',s')(\not{k}_1 + m)(\not{k}_3 + m)\gamma^+(\not{k}'_3 + m)(\not{k}_2 + m)u(p,s)\Psi(M_0'^2)\Psi(M_0^2) \ , \tag{A9}$$

$$\langle s'|J^+_{dN}(q^2)|s\rangle = p^{+2}m_N^2\mathrm{Tr}[\hat{Q}_q] \int \frac{d^2k_{1\perp}dk_1^+ d^2k_{2\perp}dk_2^+}{k_1^+ k_2^+ k_3^{+\ 2}}\theta(p^+ - k_1^+)\theta(p^+ - k_1^+ - k_2^+)$$
$$\times \mathrm{Tr}\left[(\not{k}'_3 + m)\gamma^+(\not{k}_3 + m)(\not{k}_1 + m)\right]\bar{u}(p',s')(\not{k}_2 + m)u(p,s)\Psi(M_0'^2)\Psi(M_0^2) \ . \tag{A10}$$

The normalization is chosen such that the proton charge is unity.

---

[1] G. E. Brown and M. Rho, Phys. Rev. Lett. 66 (1991) 2720.

[2] T. Hatsuda and S. H. Lee, Phys. Rev. C 46, no. 1 (1992) R34.

[3] For a review, K. Saito, K. Tsushima and A. W. Thomas, Prog. Part. Nucl. Phys. 58 (2007) 1.

[4] For a review, R. S. Hayano and T. Hatsuda, Rev. Mod. Phys. 82 (2010) 2949.

[5] For a review, W. K. Brooks, S. Strauch and K. Tsushima, J. Phys. Conf. Ser. 299 (2011) 012011.

[6] G. Krein, A. W. Thomas and K. Tsushima, arXiv:1706.02688 [hep-ph].

[7] C. R. Allton, S. Ejiri, S. J. Hands, O. Kaczmarek, F. Karsch, E. Laermann, C. Schmidt and L. Scorzato, Phys. Rev. D66 (2002) 074507.

[8] P. de Forcrand and O. Philipsen, Nucl. Phys. B673 (2003) 170.

[9] F. Cardarelli, E. Pace, G. Salme and S. Simula, Phys. Lett. B357 (1995) 267; Few Body Syst. Suppl. 8 (1995) 345.

[10] W. R. B. de Araujo, J. P. B. C. de Melo and T. Frederico, Phys. Rev. C52 (1995) 2733.

[11] A. Denig and G. Salme, Prog. Part. Nucl. Phys. 68 (2013) 113.

[12] For a review, D. F. Geesaman, K. Saito and A. W. Thomas, Ann. Rev. Nucl. Part. Sci. 45 (1995) 337.

[13] For a review, O. Hen, G. A. Miller, E. Piasetzky and L. B. Weinstein, arXiv:1611.09748 [nucl-ex].

[14] S. Strauch *et al.* [Jefferson Lab E93-049 Collaboration], Phys. Rev. Lett. 91 (2003) 052301.

[15] S. Strauch [E93-049 Collaboration], Eur. Phys. J. A 19, no. S1 (2004) 153.

[16] P. Lava, J. Ryckebusch, B. Van Overmeire and S. Strauch, Phys. Rev. C 71 (2005) 014605.

[17] D. H. Lu, A. W. Thomas, K. Tsushima, A. G. Williams and K. Saito, Phys. Lett. B 417 (1988) 217.

[18] D. H. Lu, K. Tsushima, A. W. Thomas, A. G. Williams and K. Saito, Phys. Rev. C 60 (1999) 068201.

[19] E. F. Batista, B. V. Carlson and T. Frederico, Nucl. Phys. A 697 (2002) 469.

[20] W. R. B. de Araujo, E. F. Suisso, E. F. Batista, B. V. Carlson and T. Frederico, AIP Conf. Proc. 739 (2005) 464.

[21] R. Schiavilla, O. Benhar, A. Kievsky, L. E. Marcucci and M. Viviani, Phys. Rev. Lett. 94 (2005) 072303.

[22] P. A. M. Guichon, Phys. Lett. B 200 (1988) 235.

[23] J. P. B. C. de Melo, K. Tsushima, B. El-Bennich, E. Rojas and T. Frederico, Phys. Rev. C 90 no.3 (2014) 035201.

[24] J. P. B. C. de Melo, K. Tsushima and T. Frederico, AIP Conf. Proc. 1735 (2016) 080006.

[25] J. P. B. C. de Melo, K. Tsushima and I. Ahmed, Phys. Lett. B 766 (2017) 125.

[26] K. Tsushima and J. P. B. C. de Melo, Few Body Syst. 58 (2017) 85.

[27] W. R. B. de Araújo, E. F. Suisso, T. Frederico, M. Beyer and H. J. Weber, Phys. Lett. B 478 (2000) 86.; E. F. Suisso, W. R. B. de Araújo, T. Frederico, M. Beyer and H. J. Weber, Nucl. Phys. A 694 (2001) 351.

[28] W. R. B. de Araujo, T. Frederico, M. Beyer and H. J. Weber, Eur. Phys. J. A 29 (2006) 227.

[29] W. R. B. de Araujo, T. Frederico, M. Beyer and H. J. Weber, Braz. J. Phys. 34 (2004) 251.

[30] M. K. Jones et al.[Jefferson Lab Hall A collaboration], Phys. Rev. Lett. 84 (2000) 1398.

[31] E. J. Brash, A. Koslov, Sh. Li and G. M. Huber, Phys. Rev. C 65 (R) (2002) 051001.

[32] O. Gayou et al., Phys. Rev. Lett. 88 (2002) 092301.

[33] V. Punjabi *et al.*, Phys. Rev. C 71 (2005) 055202; Erratum: [Phys. Rev. C 71 (2005) 069902].

[34] G. Ron *et al.*, Phys. Rev. Lett. 99 (2007) 202002.

[35] A. J. R. Puckett *et al.*, Phys. Rev. Lett. 104 (2010) 242301.

[36] G. Ron *et al.* [Jefferson Lab Hall A Collaboration], Phys. Rev. C 84 (2011) 055204.

[37] A. J. R. Puckett *et al.*, Phys. Rev. C 85 (2012) 045203.

[38] J. P. B. C. de Melo, T. Frederico, E. Pace and G. Salmè, Nucl. Phys. A 707 (2002) 399.

[39] H. -C. Pauli, Eur. Phys. J. C 7 (1998) 289; "DLCQ and the effective interactions in hadrons" in: New Directions in Quantum Chromodynamics, C.-R. Ji and D.P. Min, Editors, American Institute of Physics, (1999) 80-139.

[40] T. Frederico and H. C. Pauli, Phys. Rev. D 64 (2001) 054007.

[41] T. Frederico, H. C. Pauli and S. G. Zhou, Phys. Rev. D 66 (2002) 054007; Phys. Rev. D 66 (2002) 116011.

[42] J. P. B. C. de Melo, T. Frederico, E. Pace and G. Salme, Phys. Lett. B 581 (2004) 75.

[43] J. P. B. C. de Melo, T. Frederico, E. Pace, and G. Salme, Phys. Rev. D 73 (2006) 074013.

[44] E. Pace, G. Salme, T. Frederico, S. Pisano and J. P. B. C. de Melo, Nucl. Phys. A 790 (2007) 606.

[45] J. P. B. C. de Melo, T. Frederico, E. Pace, S. Pisano and G. Salme, Phys. Lett. B 671 (2009) 153.

[46] E. Pace, J. P. B. C. de Melo, T. Frederico, S. Pisano and G. Salme, Nucl. Phys. Proc. Suppl. 199 (2010) 258.

[47] S. J. Brodsky, H.-C. Pauli and S. S. Pinsky, Phys. Rep. 301 (1998) 299.

[48] F. Iachello, N.C. Mukhpadhyay and L. Zang, Phys. Rev. D 44 (1991) 88.

[49] A. V. Anisovich, V. V. Anisovich and A. V. Sarantesev, Phys. Rev. D 62 (R) (2000) 051502.

[50] S. Godfrey and N. Isgur, Phys. Rev. D 32 (1985) 189.

[51] F. Cardarelli, I. L. Grach, I. M. Narodetskii, E. Pace, G. Salmè and S. Simula, Phys. Lett. B 332 (1994) 1; F. Cardarelli, I.L. Grach, I.M. Narodetskii, G. Salmè and S. Simula, Phys. Lett. B 349 (1995) 393.

[52] H.-M. Choi and C.-R. Ji, Phys. Rev. D 59 (1999) 074015; D. Arndt and C.-R.Ji, *ibid.* 60 (1999) 094020.

[53] E. M. Aitala et al., Phys. Rev. Lett. 86 (2001) 4768.

[54] G. P. Lepage and S. J. Brodsky, Phys. Rev. D 22 (1980) 2157.

[55] S. J. Brodsky and F. Schlumpf, Phys. Lett. B 329 (1994) 111; Prog. Part. Nucl. Phys. 34 (1995) 69.

[56] F.Cardarelli and S.Simula, Phys. Rev. C 62 (2000 065201; S. Simula, nucl-th/0105024.

[57] J. Carbonell, B. Desplanques, V. Karmanov and J.-F. Mathiot, Phys. Rep. 300 (1998) 215; and references therein.

[58] J. H. O. Sales, T. Frederico, B. V. Carlson and P. U. Sauer, Phys. Rev. C 61 (2000) 044003; Phys. Rev. C 63 (2001) 064003.

[59] T. Frederico and G. A. Miller, Phys. Rev. D 45 (1992) 4207.

[60] J. P. B. C. de Melo, H. W. Naus and T. Frederico, Phys. Rev. C 59 (1999) 2278.

[61] B.L.G. Bakker, H.-M. Choi and C.-R. Ji, Phys. Rev. D 63 (2001) 074014.

[62] P. L. Chung and F. Coester, Phys. Rev. D 44 (1991) 229.

[63] W. R. B. de Araújo, T. Frederico, M. Beyer and H. J. Weber, J. Phys. G 25 (1999) 1589.

[64] W. R. B. de Araújo, T. Frederico, M. Beyer and H. J. Weber, Eur. Phys. J. A 29 (2006) 227.

[65] C. Patrignani et al. (Particle Data Group), Chin. Phys. C, 40 (2016) 100001.

[66] P. J. Mohr, D. B. Newell and B. N. Taylor, Rev. Mod. Phys. 88 no.3 (2016) 035009.

[67] J. C. Bernauer *et al.* [A1 Collaboration], Phys. Rev. Lett. 105 (2010) 242001.

[68] G. Salmé, T. Frederico and E. Pace, Few Body Syst. 56 no. 6-9 (2015) 303.

[69] J. P. B. C. de Melo, T. Frederico, E. Pace, S. Pisano and G. Salme, Phys. Lett. B 671 (2009) 153.

[70] G. Ramalho and K. Tsushima, Phys. Rev. D 84 (2011) 054014.

[71] G. Holer et al., Nucl. Phys. B 144 (1976) (505) 505.

[72] H. Y. Gao, Int. J. Mod. Phys. E 12 (2003) 1.; Erratum: [Int. J. Mod. Phys. E 12 (2003) 567.

[73] P. A. M. Guichon, K. Saito, E. N. Rodionov and A. W. Thomas, Nucl. Phys. A 601 (1996) 349; K. Saito, K. Tsushima and A. W. Thomas, Nucl. Phys. A 609 (1996) 339; Phys. Rev. C 55 (1997) 2637;
K. Tsushima, K. Saito, J. Haidenbauer and A. W. Thomas, Nucl. Phys. A 630 (1998) 691;
P. A. M. Guichon, A. W. Thomas and K. Tsushima, Nucl. Phys. A 814 (2008) 66.

[74] W. Albrecht, H. J. Behrend, H. Dorner, W. Flauger and H. Hultschig, Phys. Lett. 26B (1968) 642.

[75] S. Rock et al., Phys. Rev. Lett. 49 (1982) 1139.

[76] E. E. W. Bruins *et al.*, Phys. Rev. Lett. 75 (1995) 21.

[77] H. Anklin *et al.*, Phys. Lett. B 428 (1998) 248.

[78] G. Kubon *et al.*, Phys. Lett. B 524 (2002) 26.

[79] B. Anderson *et al.* [Jefferson Lab E95-001 Collaboration], Phys. Rev. C 75 (2007) 034003.

[80] J. Lachniet *et al.* [CLAS Collaboration], Phys. Rev. Lett. 102 (2009) 192001.

[81] T. Frederico, B. V. Carlson, R. A. Rego and M. S. Hussein, J. Phys. G 15 (1989) 297.

[82] B. D. Serot and J. D. Walecka, Adv. Nucl. Phys. 16 (1986) 1.

[83] J. R. Stone, N. J. Stone and S. A. Moszkowski, Phys. Rev. C 89 (2014) 044316.

[84] D. H. Lu, A. W. Thomas, K. Tsushima, A. G. Williams and K. Saito, Phys. Lett. B 417 (1998) 217.

[85] G. Ramalho, K. Tsushima and A. W. Thomas, J. Phys. G 40 (2013) 15102.

[86] J. Arrington, W. Melnitchouk and J. A. Tjon, Phys. Rev. C 76 (2007) 035205.

[87] M. Ostrick *et al.*, Phys. Rev. Lett. 83 (1999) 276; C. Herberg *et al.*, Eur. Phys. J. A 5 (1999) 131; D. I. Glazier *et al.*, Eur. Phys. J. A 24 (2005) 101.

[88] I. Passchier *et al.*, Phys. Rev. Lett. 82 (1999) 4988.

[89] T. Eden *et al.*, Phys. Rev. C 50 (1994) R1749.

[90] H. Zhu *et al.* [E93026 Collaboration], Phys. Rev. Lett. 87 (2001) 081801; R. Madey *et al.*

[E93-038 Collaboration], Phys. Rev. Lett. 91 (2003) 122002; G. Warren *et al.* [Jefferson Lab E93-026 Collaboration], Phys. Rev. Lett. 92 (2004) 042301.

[91] S. Riordan *et al.*, Phys. Rev. Lett. 105 (2010) 262302.

[92] R. Schiavilla and I. Sick, Phys. Rev. C 64 (2001) 041002.

[93] B. Bakamjian and L. H. Thomas, Phys. Rev. 92 (1953) 1300.